Nanopatterning of a silicon surface by near-field enhanced laser irradiation

2003 Nanotechnology 14 505

(http://iopscience.iop.org/0957-4484/14/5/305)

INSTITUTE OF PHYSICS PUBLISHING NANOTECHNOLOGY
Nanotechnology **14** (2003) 505–508 PII: S0957-4484(03)56752-6

Nanopatterning of a silicon surface by near-field enhanced laser irradiation

Y Lu and S C Chen

Department of Mechanical Engineering, The University of Texas at Austin,
1 University Station, C2200, Austin, TX 78712, USA

E-mail: scchen@mail.utexas.edu

Received 15 November 2002, in final form 27 January 2003
Published 28 March 2003
Online at stacks.iop.org/Nano/14/505

Abstract
We report on a method that allows direct, massively parallel nanopatterning of a silicon surface using ultraviolet (UV) lasers. Silica or polystyrene nanospheres with diameters of the order of the laser wavelength were deposited on the silicon surface. Spheres arranged themselves into hexagonally close-packed form due to capillary force. The nanosphere array was irradiated with 248 and 355 nm UV lasers. The silicon surface was locally melted due to enhancement of the optical field between the nanosphere and the substrate. Redistribution of molten material due to surface tension forces leads to the formation of a nanodent array. These nanodents vary their shape from bowl-like to 'sombrero-like' with the increase of laser energy as a result of competition between the thermocapillary force and the chemicapillary force.

(Some figures in this article are in colour only in the electronic version)

1. Introduction

Fabrication technologies on the nanometre scale are becoming more and more important from the viewpoint of industrial applications, for example, high-resolution lithography for the manufacture of high-density recording media, high-resolution displays or high-sensitivity biomolecule sensor arrays. Several technologies have been investigated for nanofabrication. Electron beam lithography [1] is characterized by low sample throughput, high sample cost, modest feature shape control and excellent feature size control, whereas x-ray lithography is characterized by initially high capital costs but high sample throughput [2]. Conventional photolithography has remained a useful fabrication technology due to its ease of repetition and capability for large-area fabrication. However, its minimum feature size is limited by optical diffraction [3].

To circumvent the diffraction limit, near-field photolithographic techniques have been developed for nanostructuring by delivering a laser beam through a hollow near-field tip or illuminating the tip of a scanning probe microscope with a pulsed laser [4, 5]. A strong local optical field is established between the sample surface and the sharp tip when the surface-to-tip gap is a few nanometres. Structures with lateral dimensions below 30 nm, and therefore well below the minimal resolvable feature size of half a wavelength of the light, were produced underneath the tip [6]. However, this kind of near-field nanolithographic technique has rarely been used in an industrial setting due to its limited throughput, hollow tip blockage and difficulty in process control.

Motivated by the problem of structure damage in dry laser cleaning of submicron particles on surfaces [7], a new approach involving the illumination of nanometre-sized spheres using a laser beam was recently demonstrated to pattern a solid surface on a nanoscale [8–10]. A spherical particle may act as a lens and therefore intensify the incoming laser beam if the diameter of the sphere is larger than the laser wavelength. Near-field enhancement may play an important role if the diameter of the nanosphere is equal to or smaller than the wavelength.

In this study, a monolayer of self-organized hexagonally close-packed nanospheres made of silica or polystyrene is used to pattern a silicon surface in a massively parallel fashion. The laser intensity is controlled to investigate the dependence of surface topography on laser energy. The morphologies of the features produced on the silicon surface are characterized by an atomic force microscope (AFM) and a scanning electron microscope (SEM). The near-field effect in laser–nanosphere interactions and the surface tension effect responsible for surface pattern formation are discussed in detail to reveal the physics of the surface nanopatterning process.

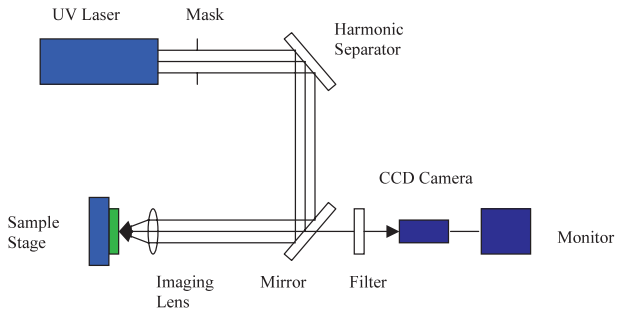

Figure 1. Experimental set-up for laser nanopatterning of a silicon surface.

2. Experiments

Surface polished n-type silicon wafers of (100) crystal orientation were used as the substrate. To clean them, the silicon substrates were sonicated in water and subsequently in isopropyl alcohol. This type of silicon wafer has a native oxide layer with a stoichiometry close to SiO_2 and a thickness of 2–3 nm. Two types of nanosphere were used in this work: polystyrene (diameter = 560 nm) and silica (diameter = 640 nm). Methods for deposition of a solution of nanospheres onto the desired substrate include spin-coating, drop coating and thermoelectrically cooled angle coating [11–13]. All of these deposition methods require that the nanospheres are able to freely diffuse across the substrate, seeking their lowest-energy configuration. After dropping an aqueous solution of monodispersed polystyrene or silica spheres onto the substrate, water was evaporated from the solution in a chamber under controlled humidity. As the solvent evaporates, capillary forces draw the nanospheres together, and the nanospheres reorganize themselves in a hexagonally close-packed pattern on the substrate. The as-deposited nanosphere array may include a variety of defects that arise as a result of nanosphere polydispersity, site randomness, point defects and line defects. Before being exposed to a laser, the surface of the sample was characterized by SEM.

As shown in figure 1, samples were irradiated with the third harmonic wave of an Nd:YAG laser (λ = 355 nm, FWHM = 10 ns) or a KrF excimer laser (λ = 248 nm, FWHM = 10 ns), which generates nanosecond pulses. The laser beam was focused by a lens (f = 50.8 mm) onto the samples mounted on a three-dimensional precision stage. Different laser intensities were used to study the laser energy dependence of the nanofeatures. All experiments were performed under ambient conditions. Finally the laser-patterned silicon surface was observed by SEM and AFM.

3. Results and discussion

3.1. Resulting images

SEM images of the substrate surface with patterned nanospheres before laser irradiation are shown in figure 2. Both silica nanospheres of diameter 640 nm (figure 2(a)) and polystyrene nanospheres of diameter 560 nm (figure 2(b)) formed a monolayer on the Si substrate with a hexagonally close-packed arrangement.

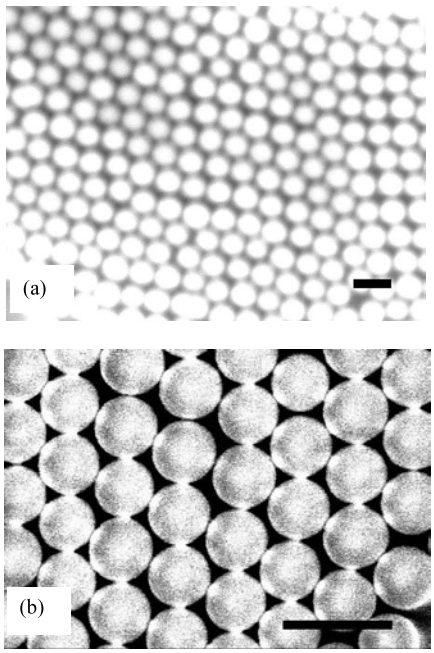

Figure 2. SEM images of a hexagonally close-packed monolayer of (a) polystyrene nanospheres of diameter 560 nm and (b) silica nanospheres of diameter 640 nm on a silicon substrate. The scale bar indicates 1 μm.

After laser irradiation, labelled areas on the silicon surface were observed under SEM and compared with images taken before laser irradiation. Most of the spheres disappeared, while dent structures with the same hexagonal pattern as the spheres were formed on the silicon surface. Figure 3(a) shows those dent structures with a polystyrene sphere still present on one of the dents. A similar phenomenon is observed in figure 3(b) where the spheres still remain at the monolayer edge and adjacent dents are aligned in a hexagonal arrangement. This indicates that the nanodent structures were produced underneath the spheres.

As measured by AFM, the sizes of the dents as a function of the laser energy delivered onto the substrate are summarized in figure 4. In both cases, i.e. using silica and polystyrene nanospheres, the diameter of the dent increases with the laser energy, but this trend becomes less significant at higher laser intensities. We observed one interesting phenomenon: at the lower laser energy only bowl-type dents were produced on the silicon surface (figure 5(a)), while at the higher laser intensity, 'sombrero'-type bumps were formed, as shown in figure 5(b). AFM measurement confirmed that a central peak was surrounded by an outer ring, as depicted in figure 6.

3.2. Near-field enhancement

The optical enhancement by nanospheres in the near-field region can be explained by Rayleigh scattering and Mie scattering. Rayleigh scattering takes place when the diameter of the sphere is less than the wavelength of the light. In this case, the sphere is treated as dipole radiator. When the diameter of the sphere is equal to or greater than the wavelength, light is scattered elastically according to the Mie scattering law.

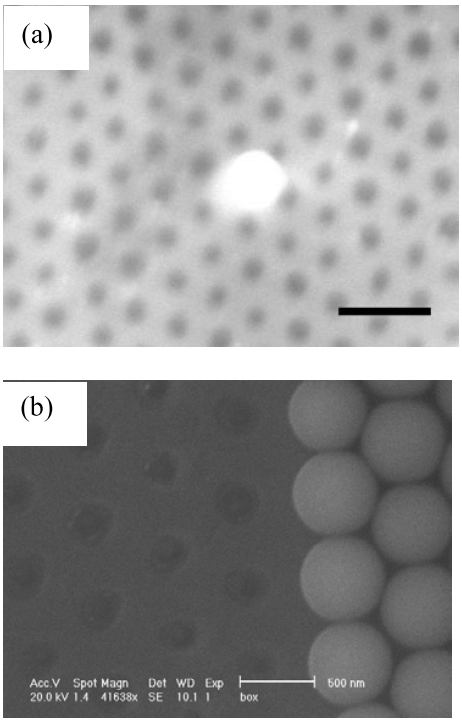

Figure 3. SEM image of hexagonally arranged dent structures: (a) with a polystyrene sphere sitting on the dent (the scale bar indicates 1 μm); (b) with a line of nanospheres at the edge indicating that the nanostructure was produced underneath the nanosphere. The laser fluence for both cases was 4 mJ cm^{-2}.

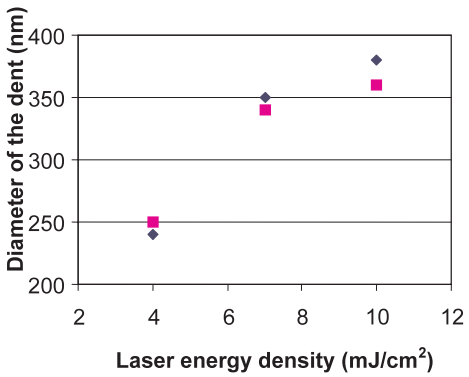

Figure 4. The laser energy dependence of dent diameters: ♦, 640 nm silica spheres with a 248 nm KrF excimer laser; ■, 560 nm polystyrene spheres with a 355 nm Nd:YAG laser.

It has been reported that the intensity distribution changes dramatically with the size of the sphere and also the distance between the sphere and the substrate [9, 10]. A Rayleigh sphere (sphere diameter less than the laser wavelength) enhances the electric field at its sides along the direction of polarization of the incident light. It can hardly focus the incident light due to the diffraction limit. In contrast, the electric field around a Mie sphere (sphere diameter larger than the laser wavelength) is enhanced by several times towards the forward area of the sphere [10]. Such optical enhancement will lead to local melting or even vaporization of the substrate materials for nanoscale surface patterning.

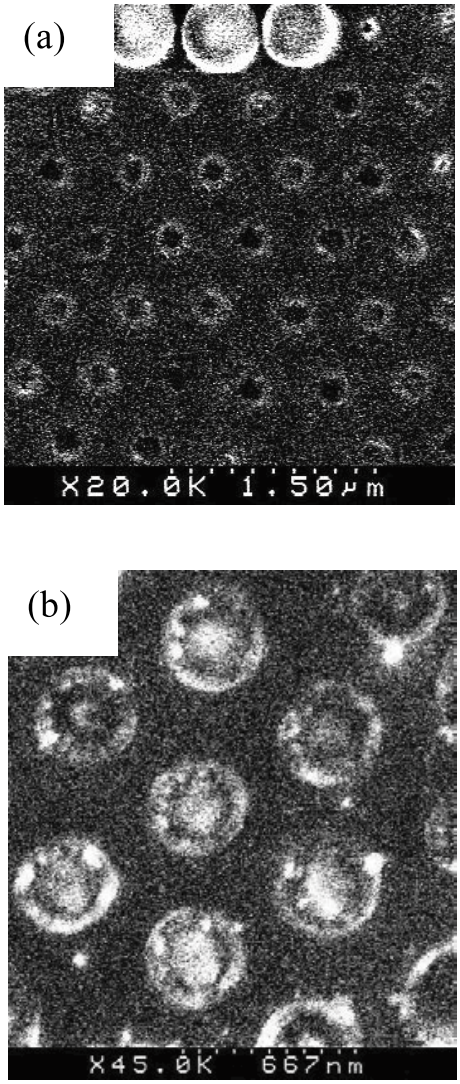

Figure 5. SEM images of hexagonally arranged dent structures, (a) bowl type and (b) 'sombrero' type, produced using silica nanospheres upon irradiation with a 248 nm KrF excimer laser. The laser fluence delivered was 4 mJ cm^{-2} for (a) and 10 mJ cm^{-2} for (b).

3.3. Hydrodynamic mechanism for topography formation

In general, the possible forces giving rise to the motion of the laser-heating-induced melt can be categorized as either body or surface forces. The static force of gravity is recognized as insignificant on a nanometre scale. However, an inertial force which could arise from elastic motion of underlying material might be considered. An inertial force acting on the melt will arise from a non-zero coefficient of thermal expansion. As shown in figure 5, at low pulse energy there is a depletion of material from the central region, while at higher pulse energy there is an accumulation of material at the centre. While the magnitude of inertial forces acting on the molten layer changes with pulse energy, the direction does not.

Surface forces include both normal and shear stress. Normal stress may arise in the problems due to the surface recoil pressure of vaporized material or the Young–Laplace pressure discontinuity across a curved interface. Previous work on laser texturing of NiP and silicon materials has

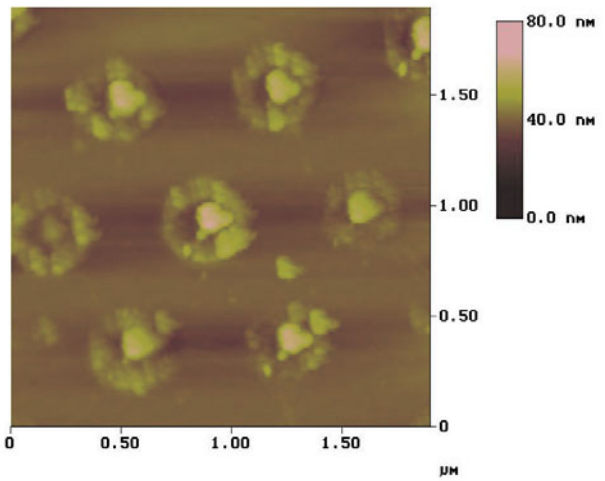

Figure 6. AFM image of dent structures formed under 640 nm silica nanospheres after irradiation by a 248 nm KrF excimer laser, indicating a clear central peak surrounded by an outer ring. The laser fluence delivered was 10 mJ cm^{-2}.

demonstrated that Marangoni-driven flow is considered to be mainly responsible for the redistribution of surface material upon laser melting on a microscale, although secondary effects due to surface curvature and vapour recoil pressure are included [14–16]. The Marangoni effect, which involves shear stress, refers to the motion of liquid due to surface tension gradients. Thermocapillarity and chemicapillarity are believed to be two distinct components, which result from the thermal potential of a temperature gradient and the chemical potential of a compositional gradient respectively. The thermocapillary force acts to move the material towards cooler regions of higher surface tension, which is true for most pure liquids. The chemicapillary force acts to move material toward regions of higher surface energy corresponding to lower surfactant concentration. The surface compositional gradient may arise from the depletion of a surfactant, such as SiO_2 in this work. If local depletion of the surfactant is sufficient, the resulting chemicapillary action will also contribute to the redistribution of molten material.

The experimental data show that there exists a threshold energy for the formation of a central peak, below which only a bowl-shaped bump forms. This threshold energy is related to SiO_2 vaporization, below which the thermocapillary force redistributes the molten material in the absence of a compositional gradient at the surface. Due to the Gaussian-like distribution of the enhanced optical field [8], the temperature decreases from the centre of the molten zone to its edge. This temperature gradient results in outward flow which is responsible for the formation of the outer rim and the bowl-type nanostructure. However, when the central peak energy of the laser exceeds the activation energy for significant vaporization of the natural SiO_2 layer, which is only a few nanometres thick, depletion of SiO_2 introduces chemicapillary action. The highest surface tension exists at the centre of the molten zone due to the strongest SiO_2 depletion. Therefore, the molten material flows inward towards the centre where chemicapillary force dominates, while retaining the same trend for the ring formation near the edge because the laser energy is still not high enough to evaporate SiO_2 there.

4. Conclusion

We have shown that it is possible to utilize the optical near-field properties of nanospheres to pattern a silicon surface in a massively parallel fashion. A monolayer of silica and polystyrene nanospheres was deposited on the silicon surface by self-assembly. Nanosized dent structures were produced underneath the spheres upon UV laser irradiation through the nanosphere layer. Mie scattering was found to be the dominant mechanism for the optical field enhancement for sphere size larger than the laser wavelength. The dent topography was explained by the Marangoni effect, surface deformation mainly being due to competition between the thermocapillary and chemicapillary forces. Other effects such as recoil pressure and resonance of the nanospheres may make a contribution to the surface nanopatterning. Further investigations are necessary to evaluate these effects. Although nanostructures produced in this work are of the order of 300 nm, we expect that finer patterns can be produced by the use of smaller nanospheres.

Acknowledgments

This work was supported by a CAREER award to S C Chen from the US National Science Foundation. The authors wish to thank Dr G C Wilson for the excimer laser support and Dr P S Ho for the AFM use. The SEM measurement was conducted at the Texas Materials Institute at the University of Texas at Austin.

References

[1] Cumming D R S, Thoms S, Beaumont S P and Weaver J M R 1996 *Appl. Phys. Lett.* **68** 322
[2] Smith H I and Schattenburg M L 1993 *IBM J. Res. Dev.* **37** 319
[3] Madou M 2002 *Fundamentals of Microfabrication* 2nd edn (Boca Raton, FL: Chemical Rubber Company Press)
[4] Betzig E and Trautman J K 1992 *Science* **257** 189
[5] Ohtsu M and Hori H 1999 *Near-Field Nano-Optics* (New York: Kluwer Academic)
[6] Lu Y F, Mai Z H, Qiu G and Chim W K 1999 *Appl. Phys. Lett.* **75** 2359
[7] Mosbacher M, Munzer H J, Zimmermann J, Solis J, Boneberg J and Leiderer P 2001 *Appl. Phys.* A **72** 41
[8] Huang S M, Hong M H, Lu Y F, Luk'yanchuk B S, Song W D and Chong T C 2002 *J. Appl. Phys.* **91** 3268
[9] Watanabe O, Ikawa T, Hasegawa M, Tsuchimori M and Kawata Y 2001 *Appl. Phys. Lett.* **79** 1366
[10] Munzer H J, Mosbacher M, Bertsch M, Zimmermann J, Leiderer P and Boneberg J 2000 *J. Microsc.* **202** 129
[11] Hulteen J C and Van Duyne R P 1995 *J. Vac. Sci. Technol.* A **13** 1553
[12] Hulteen J C, Treichel D A, Smith M T, Duval M L, Jensen T R and Van Duyne R P 1999 *J. Phys. Chem.* B **103** 3854
[13] Micheletto R, Fukuda H and Ohtsu M 1995 *Langmuir* **11** 3333
[14] Chen S C, Cahill D G and Grigoropoulos C P 2000 *J. Heat Transfer* **122** 107
[15] Bennett T D, Krajnovich D J, Grigoropoulos C P, Baumgart P and Tam A C 1997 *J. Heat Transfer* **119** 589
[16] Schwarz-Selinger T, Cahill D G, Chen S C, Moon S J and Grigoropoulos C P 2001 *Phys. Rev.* B **64** 155323